LRP 378/89   June 1989

CONTROL, PRESSURE PERTURBATIONS, DISPLACEMENTS, AND DISRUPTIONS IN HIGHLY ELONGATED TOKAMAK PLASMAS

F.B. Marcus, F. Hofmann, S.C. Jardin, P. Noll
and G. Tonetti

CONTROL, PRESSURE PERTURBATIONS, DISPLACEMENTS, AND DISRUPTIONS IN HIGHLY ELONGATED TOKAMAK PLASMAS

F.B. MARCUS*, F. HOFMANN, S.C. JARDIN**, P. NOLL***, G. TONETTI

Centre de Recherches en Physique des Plasmas
Association Euratom - Confédération Suisse
Ecole Polytechnique Fédérale de Lausanne
21, Av. des Bains, CH-1007 Lausanne, Switzerland

ABSTRACT

The control and evolution of highly elongated tokamak plasmas with large growth rates are simulated with the axisymmetric, resistive MHD code TSC in the geometry of the TCV tokamak. Pressure perturbations such as sawteeth and externally programmed displacements create initial velocity perturbations which may be stabilized by low power, rapid response coils inside the passively stabilizing vacuum vessel, together with slower shaping coils outside the vessel. Vertical disruption induced voltages and forces on the rapid coils and vessel are investigated, and a model is proposed for an additional vertical force due to poloidal currents.

*   Present address: JET Joint Undertaking, Abingdon, Oxfordshire, England

**   Plasma Physics Laboratory, Princeton University, Princeton, N.J., U.S.A.

***   JET Joint Undertaking, Abingdon, Oxfordshire, England

1. INTRODUCTION

Existing tokamak experiments have been built and future tokamak fusion reactors are being designed with plasmas which are highly elongated to maximize current, pressure, and confinement time, but which are also vertically unstable and require feedback control. In this paper, we investigate the effects of pressure perturbations on control of these plasmas and on the evolution of disruptions which affect the design of the control system and coils.

It has been shown (1) with the axisymmetric, resistive MHD code TSC (2) that tokamak plasmas may be evolved to high elongation. However, these elongated plasmas are vertically unstable. The stabilization of this ideal, axisymmetric mode requires a passive stabilizer close to the plasma (3,4,5). As a particular example, passive stability has been studied for plasmas in the geometry of the TCV tokamak (4) under construction at the CRPP. TCV has a maximum design current of 1200 KAmps, plasma half-width $a_0 = 0.24$ m, half-height $b_0 = 0.72$ m, major radius $R_0 = 0.87$ m, toroidal field $B_0 = 1.43$ T, and pulse length at full field about 1 sec. The TCV vacuum vessel is used as a continuous passive stabilizer with inside half-width = 0.28 m, inside half-height = 0.77 m, resistance = 50 μohms, and time constant (m=1) = 6.7 msec. In (3,4,5), the stability to ideal axisymmetric modes has been investigated using the FBT and ERATO codes. As elongation or the plasma-wall distance is increased, a broader current profile, and therefore, with a fixed safety factor q_0 on axis, a minimum current is required for stability. Dee plasmas tend to be more stable than racetracks. The resistive axisymmetric growth rate for TCV plasmas due to vessel resistivity and studies on plasma control have been described in (6,7,8,9).

In addition to these minimum current limits, there are maximum current and pressure limitations due to ideal non-axisymmetric modes, such as kink modes (9,10,11). These studies show that in order to operate tokamaks having an aspect ratio similar to TCV with elongation greater than $\kappa=2/1$, it is necessary to be in a restricted range between the minimum and maximum current.

Experimental studies of the vertical instability growth rate in moderately elongated tokamaks have been made in several tokamaks. Stable plasmas with surface elongations κ of up to 1.8 (aspect ratio 3.4) have been produced in the upper lobe of Doublet III with the use of both passive and active controls (12), up to 2.0 with an in-situ pellet (13), and greater than 2.0 in the lower aspect ratio DIII-D (14). In a study of growth rates with the feedback turned off (12) in Doublet III, growth rates of $(2-20 \text{ msec})^{-1}$ were observed for elongations up to 1.8, all slower than the inverse of the vessel time constant (approx. 1 msec). The coils just outside the vessel act both as passive and active stabilizer. The maximum growth rate which can be controlled is $(4 \text{ msec})^{-1}$, consistent with their thyristor power supply response time. In the experiment JFT-2M, with plasma elongations up to $\kappa=1.7$, resistive vertical growth rates up to $(2 \text{ msec})^{-1}$ have been controlled (15). In this case, the growth rates are faster than the inverse of the time constant of 7 msec for the vessel, which is effective in stabilizing the plasma. The $(2 \text{ msec})^{-1}$ limit is approximately the inverse of the time interval between thyristor firing in their 12 pulse

2

system at 50 Hz. Simulations have been made (16) of control with thyristor supplies using a simplified plasma model in a different geometry.

In what follows, we use the TSC code, which has been verified against both analytic calculation and full simulations of evolution and disruptions in tokamak plasmas (2,17), to study the response of elongated plasmas to pressure perturbations and externally programmed motion. The goal is to investigate the sources of plasma axisymmetric instability and to demonstrate solutions which are generally applicable in elongated tokamaks. In Section 2, the method of calculating the resistive axisymmetric growth rates of plasmas in TCV geometry is discussed, in the absense of feedback control. The sources of plasma perturbations and effect of pressure drops on initial position and velocity are investigated. In Section 3, we discuss a control system using coils inside the vacuum vessel which are used to control the plasma in the presence of these perturbations. In Section 4, we investigate two time scale control, studying the interaction of the slower coils outside the vacuum vessel with the fast coils inside, and the limits of control with outer coils.

A study is included in this paper on the effects of disruptions on the fast control coils inside the vessel and their power supplies, and on the vessel forces from the loss of these highly elongated and unstable plasmas which can be formed with this control system. In Section 5, the induced voltages, currents and forces due to plasma disruptions are calculated, when the plasma excursions are too large to be controlled. In Section 6, a model is proposed for an additional vertical force due to poloidal current flowing from the plasma into the vessel, which could be included in a self-consistent simulation. The summary and conclusions are presented in Section 7.

2.   PERTURBATIONS AND AXISYMMETRIC RESISTIVE GROWTH RATES

The computer program used in the following simulation studies is called TSC, the Tokamak Simulation Code (2). It models the 2D axisymmetric resistive instability and control of tokamak plasmas, and has been validated against measurements in the tokamaks TFTR, DIII-D, and PBX, for experiments on plasma evolution, control, and disruptions. It solves the Maxwell-MHD equations in three regions: plasma, vacuum, and active and passive conductors. Circuit equations, including feedback systems, are solved for the poloidal field coils. In the plasma, the mass is artificially enhanced, and the momentum equation evolves velocity and enforces force balance. The mass enhancement factor must be small enough to give a good separation between ideal and resistive time scale motion, but not too small, otherwise computational time becomes excessive. The Alfven time and computational time are proportional to the square root of this factor. In the simulations in this paper, this factor and other numerical solution parameters were varied to verify the convergence and accuracy of the results.

Resistive growth rates are calculated with TSC as follows: The equilibrium to be studied is specified with shaping coil currents, plasma current profile, limiters, and shape control moments. An equilibrium is calculated, and the voltage applied to the shaping coils is only the resistive voltage, without feedback. The elements of the passively stabilizing vacuum vessel are

3

resistive short circuits. The plasma then evolves in time, and both the height of the magnetic axis and the flux difference between the plasma top and bottom are observed to measure the resistive axisymmetric growth rate. For dee or racetrack plasmas with elongations of 2/1 or greater, and a plasma-wall gap of at least 0.04 m in TCV geometry, the growth rates exceed $(1 \text{ msec})^{-1}$, compared to the inverse of the vessel time of 6.7 msec. In this regime, the shaping coils external to the vessel do not affect the growth rate, whether they are treated as passive short-circuits or as fixed current sources. Without a vacuum vessel, the instability grows many times faster than the resistive growth rate. With the vessel present, the plasma may be either ideally stable or unstable, depending on elongation, plasma-wall gap, and current profile. A 3/1 elongated dee-shaped plasma in TCV with 1200 KAmp and a 0.04 m plasma-wall gap has a converged growth rate of $(0.2 \text{ msec})^{-1}$.

For the design of a feedback control system, it is not sufficient to know only the plasma growth rate, which will determine the minimum frequency response of the feedback amplifier. In particular, the maximum voltage, current, and response time required of the amplifier depend on the initial perturbation to be controlled, in terms of plasma velocity and growth rate. These initial perturbations can arise from several sources: internal sawteeth; minor or major disruptions leading to pressure loss; apparent perturbation from a difference between actual and programmed plasma motion; and apparent perturbations from MHD activity and noise influencing magnetic probe measurements of the plasma position.

An example of the effect of giant sawteeth oscillations is shown in data from shot 33899 in Doublet III, see Fig. 5 in ref. (18). Sawteeth activity in an auxiliary-heated, high-beta plasma causes pressure and radial position variations. The plasma has a 1.58/1 elongation and toroidal beta of 3%. The pressure, as shown by the poloidal beta trace, oscillates by about 1/6 of its maximum value, and the radial position oscillates 0.010 - 0.015 m, resulting in velocities of about 10 m/sec.

Apparent perturbations occur due to preprogrammed motion of the plasma. In TCV, one operating scenario is to start the plasma near the top of the vessel to maximize wall stabilization, and then to elongate by moving the plasma lower boundary downwards. With the vessel dimensions and the tokamak experimental time scales, induced velocities of up to 10 m/sec may be programmed. Apparent perturbations due to MHD activity may result from lack of compensation of n=1 (or greater) signal pickup, or from n=0 activity. There are too many types of MHD modes to consider here, but very rough estimates based on perturbed magnetic fields give inferred maximum velocities of 10^0-10^1 m/sec.

Guided by the above, pressure loss is simulated in TCV geometry with the TSC code, to determine resulting vertical velocities. In Fig. 1a, a 2.2/1 elongated, single-null divertor equilibrium is shown in TCV geometry, with 16 shaping coils outside the vessel, which is modeled by many continuous passive conductors. The plasma current of 500 KAmps and the fractional pressure drop of 1/6, from 5.8% to 4.8% toroidal beta, are chosen to be similar to the Doublet III sawtooth example. The before and after radial profiles of pressure are shown in Fig. 1b. In the absence of feedback control, the time response of the position of the plasma magnetic axis is shown

in Figs. 1c and 1d. As a result of the pressure drop between time= 0.20 and 0.25 msec, the radial position xmag decreases by 10 mm and the vertical position zmag decreases by 5 mm. The 0.05 msec is characteristic of thermal quench times (17) rather than of sawteeth, which gives a clear separation between position jumps and exponential growth. In this non-symmetric plasma, the radial position jump caused by a pressure loss couples to a jump in vertical position. Although the radial motion stops after the jump, the plasma has acquired a vertical velocity of 10 m/sec. Further simulation shows that the initial vertical position displacement and velocity continue to increase at the growth rate of $(0.8 \text{ msec})^{-1}$. These values impose requirements on the voltage and current and response time of the feedback system.

3.   CONTROL OF PERTURBATIONS WITH COILS INSIDE THE VACUUM VESSEL

The high current shaping coils outside the TCV vessel have 12 pulse thyristors driven by a 96-120 Hz generator, and can control growth rates up to about $(1 \text{ msec})^{-1}$, corresponding to plasmas up to about 2/1 elongation (7). To improve the operating range of TCV, coils with low current, fast response power suplies are added inside the vessel, at large major radius, at the top and bottom corners (see Fig. 1a, shaded coils), with opposite polarity to create a radial field for vertical instability control.

To compare the relative efficiency of coils inside versus outside the vessel, coils were placed either one grid spacing (0.025m) inside or outside the vessel wall, and a square voltage pulse applied for 0.2 msec, corresponding to the the maximum growth rate studied. In the absence of plasma, the flux difference between the points R=0.87m, z=+-0.72m, (measuring the radial field) is an order of magnitude greater from the inside coils, even with similar coil currents. The measured flux due to the inside coils is proportional to current in the inner coils, but the flux from the outer coils is delayed and attenuated on this time scale.

This difference in radial flux production may be understood as folows: Coils inside the vessel produce a "prompt" flux in the plasma region which is the leakage flux squeezed between the coil and the image currents in the wall. On a short time scale, this flux dominates the net flux due to decay of image currents in the wall. The flux produced by coils outside the vessel is delayed and attenuated by resistive decay of image currents in the vessel, since the "prompt" flux inside is zero. The skin effect due to finite vessel wall thickness is not considered. It can only worsen the efficiency of coils outside the vessel.

For coils inside the vessel, flux production increases with increasing coil to wall gap, but there are technological constraints: Disruption induced voltages and currents also increase with the gap size (see section 5). Space must be allowed for a gap to the plasma, and for coil supports and protection.

With these fast coils inside the vessel, the TSC code is used to determine the feedback control requirements in the presence of plasma perturbations. These coils are (separately) connected to linear amplifiers (no time delay), and their applied voltage V is calculated by a proportional - differential (PD) controller on the vertical position flux error,

$$V = P \ (\ (\psi_1 - \psi_2) + D \ (d/dt) \ (\psi_1 - \psi_2) \ ) \ + I_c R_c \ ,$$

where ψ_1 and ψ_2 are fluxes measured at fixed points near the top and bottom of the plasma outer flux surface at major radius = 0.91m, P = 400 Kvolts / (weber/radian), D = 0.2 msec, $I_c R_c$ is the coil resistive voltage, and opposite polarity voltages are applied to the top and bottom coil. A single-turn maximum voltage of 50 volts/turn is imposed as a maximum (non-linear) limit on these linear amplifiers. Three values of the single turn resistances R_c of the coils are considered, 5.0 and 2.5 mohms, normal values with protected copper winding, and 0.05 mohms, a small value for demonstration.

An example is shown in Fig. 2 of feedback control using only rapid coils inside the vessel in the presence of a plasma pressure perturbation. Using the same equilibrium as in Fig. 1a, the ratio of plasma pressure to toroidal field pressure, β, is dropped from 5.8% at 0.20 msec to 5.3% at 0.25 msec, with a resistance of 5 mohms in each feedback coil. The vertical position of the magnetic axis versus time is shown in Fig. 2a, and the applied voltage and resulting current waveforms of the upper feedback coil are shown in Figs. 2b, 2c. During the first 0.2 msec, the radial and vertical positions evolve slightly as the feedback system is turned on and as the initial numerical conditions of the MHD equilibrium evolve resistively, especially at the cold edge. From 0.20 to 0.25 msec, the pressure decrease of $\Delta\beta$ = 0.5% causes the plasma to jump inwards by 4 mm, and then evolve slowly afterwards to a final change of 6 mm. The vertical position jumps downwards and continues moving. The voltage on the feedback coil is driven to its maximum positive voltage, and the coil current increases rapidly by about 6 KAmp until the vertical position is stabilized, after about 0.40 msec, then increases another 1 KAmp more slowly, for a total of 7 KAmp. Since no filtering of the flux measurement is used, the derivative term in the PD controller can lead to voltage jumps, for example at 2.75 msec.

Referring to Fig. 2a, two other simulations were made for comparison: If the feedback is turned off at the time 0.2 msec when the pressure drop begins, then the evolution of the vertical position is nearly identical until 0.35 msec, but then continues negative and grows exponentially, as in Fig. 1d; If the feedback is left active, but no pressure jump occurs, then the vertical position is stabilized between 72.1 and 72.4 mm, after the time 0.2 msec.

The scaling of the required voltages, currents, and jumps is shown by four examples in Table I, including data from Fig. 2. In the first 3 cases, the changes after 1-2 msec in radial position ΔR, vertical position Δz and feedback coil current ΔI_c increase with the jump in pressure ratio $\Delta\beta$ during the jump time Δt_J. The coil resistance R_c in the third case is reduced to avoid the 10 KAmp resistive saturation at 50 volts. The higher the current, the longer the time to reach equilibrium, since the current increase at 50 volts is limited by the effective high-frequency self-inductance of 4 μH of the fast coil in the presence of the vessel. Although 0.05 msec is characteristic of the pressure loss during a disruption, the drop in the pressure during a

sawtooth, as seen in the poloidal beta oscillations (18), occurs on the msec time scale. In the last case in Table I, the jump time is increased to the sawtooth time scale of 1.0 msec, comparable to the time required to reach the coil current maximum. In this case, the coil voltage stays near 50 volts, but does not saturate. The coil current jump is reduced to 11 KAmp, and is reached at the same time as the jump finishes. In conclusion, to control sawtooth-like perturbations, power supplies are required with about +-50 volts/turn and +- 10 KAmp-turn in TCV geometry.

Several other plasma configurations have been studied with this stabilization system of coils in the vessel corners. It is possible to stabilize centered (vertically) and non-centered, up-down symmetric and non-symmetric plasmas with very high growth rates much greater than $(1 \text{ msec})^{-1}$, for example with 2/1 and 3/1 elongated dees, racetracks, and single-null divertors. The result is that even with coils only in the corners, which produce an up-down symmetric, highly distorted field in the presence of the vessel, the plasma motion can be stabilized, without visible plasma distortion. Also, higher order axisymmetric modes for plasmas up to 3/1 elongation are not observed to be dangerous on the time scale of a few msec.

4.   TWO TIME SCALE CONTROL

Pressure perturbations in non-symmetric plasmas can lead to vertical velocities of 10 m/sec. In this section, we investigate the programmed motion and stabilization of a highly unstable, 3/1 elongated dee plasma with 1200 KAmps and a growth rate in the absence of feedback of $(0.3 \text{ msec})^{-1}$. An initial equilibrium is calculated with TSC, shown in Fig. 3. The flux point defining the desired bottom of the plasma is commanded to move upwards at 10 m/sec, while the plasma touches a fixed limiter at the top. This command corresponds to an apparent perturbation.

A simulation was made with only the fast coils inside active and the shaping coils outside the vessel short-circuited, with shaping currents present. In response to the moving flux reference at the bottom of the plasma, the voltage on the coil at the bottom goes immediately to the limit of -50 volts (+50 volts on the upper coil) due to the controller derivative term, to start the plasma moving vertically. The coil current also goes in the negative direction. Once the plasma starts moving upwards at the programmed 10 m/sec, it tries to go vertically unstable at the resistive growth rate. The applied feedback voltage changes sign to restrain this vertical acceleration, and the direction of the coil current changes. During the first msec, the plasma moves smoothly upwards, following the command, and behaves as in Figs. 4a, b, c described in the following paragraph. However, during the period 1.0 to 1.5 msec, the coil voltage reaches its maximum +50 volts, but the coil current is resistively limited to 10 KAmps for $R_c = 5$ mohms. After 1.5 msec, because of this saturation, the control of the plasma is lost, and the plasma accelerates upwards with the resistive growth rate.

The fast coils inside the vessel, with their limited current and voltage, cannot maintain sustained plasma displacements. To control plasmas over both short and long time scales, the fast coils inside and slow coils outside the vessel must be programmed to work together. An example is shown in Fig. 4, where as in the previous discussion, the flux point defining the desired plasma

7

bottom is programmed to move upwards, and the fast coils inside the vessel have PD voltage control. In addition, the slower shaping coils at large major radius have a voltage applied which is proportional to the current in the fast coils inside the vessel. For this example, the proportionality constant is the fast coil resistance, here reduced to 2.5 mohms, giving a maximum command voltage of 25 volts/turn, corresponding nearly to the thyristor supply limits on shaping coils at large major radius. The four shaping coils above the midplane at large major radius have the opposite voltage applied to those below the midplane, producing an approximately radial field. The result of this feedback scheme is that current flowing in the slower coils will produce a field which replaces the field from the faster coils, thereby reducing the fast coil current.

The plasma and coil geometry are the same as in Fig. 3. The snapshots of the lower portion of the outermost flux surface show the bottom of the plasma moving linearly upwards in Fig. 4a during 5.5 msec of evolution. The top is fixed on an upper limiter. In Figs. 4b, the bottom fast coil voltage goes negative to push the plasma upwards, then positive to restrain it. In Fig. 4c, the fast coil current responds accordingly. The shaping coils at small major radius have a command voltage set equal to their own resistive voltage. The coils at large major radius are commanded as described to produce a radial field, with voltage on the bottom coil shown in Fig. 4d and current in Fig. 4e. The thyristor nature of the supplies is evident. After 2 msec, the outer coils' flux limits the current required from the inner coils to 10 KAmp-turns per coil. Since there are 8 slow coils with a low resistance compared to the two fast coils, the flux from the external coils and the resistance in the fast coils inside the vessel causes the fast coil current to decrease as desired. In Fig. 4f, the vertical position of the magnetic axis is shown. The magnetic axis starts to move at 10 m/sec, the same velocity as the plasma bottom, but then slows down. This shows the deformable nature of the plasma (which can effect feedback stability (19)), since with a fixed upper limiter, on average the magnetic axis can move only half the distance with half the velocity of the plasma bottom.

The method chosen here for controlling the slower shaping coils is only one of many possibilities. For example, as in (1,7), both small and large major radius shaping coils may be used together to create an optimum radial feedback field, and current instead of voltage control may be used for the thyristors. Also, the crossover time of the fast and slow system found here of 1-2 msec is consistent with the result (7) that growth rates of about $(1 \text{ msec})^{-1}$ are the maximum controllable with 96 Hz, 12 pulse thyristors. At high frequency, the effective self inductance of the fast coil in the presence of the vessel of 4 μH and the chosen coil resistance give a 1.6 msec time constant, comparable to the crossover time.

Other control methods were attempted which were not successful for high growth rate plasmas. Applying the same voltage to both fast and slow coils from a PD controller on the plasma edge flux did not work, because large voltage jumps were induced in the thyristor supply response, which require a full half cycle at 96 Hz to recover. Also, attempts with fast coils outside the vessel did not work because of delays and phase shifts of fields penetrating through the vessel.

In conclusion, pressure or apparent perturbations due to programmed motion, both

8

corresponding to a 10 m/sec velocity, can be controlled with the coils and power supply parameters used here, and these methods can be applied generally to tokamak control problems.

5.   PLASMA DISRUPTION INDUCED VOLTAGES AND FORCES

When a perturbation is too large to be controlled, as in a major disruption (17), the resulting plasma evolution can produce large voltages and induced currents and forces on the fast coils and vacuum vessel. In this section, we investigate two effects of a rapid, vertical plasma disruption: voltages and induced currents in the fast coils inside the vessel; and net vertical forces, including an additional force from poloidal currents flowing from the plasma into the vessel.

If a plasma pressure perturbation is too large to control, a plasma will go vertically unstable, inducing large voltages inside the vessel and currents in the vessel and the fast coils inside (depending on protection circuitry). An example of a rapid current loss and vertical disruption is shown in Fig. 5. To create conditions in which the disruption time (approx. 1 msec) is much less than the vessel time (approx. 7 msec), the plasma pressure is decreased by dropping the electron temperature to 10 eV, and the inner vessel wall is moved an additional 25 mm from the plasma, towards small major radius. Such low electron temperatures are observed to result from disruptions (17,20). As is seen from Fig. 5a, with snapshots of the outermost flux surface, the plasma moves upwards at the same time as the current falls, see Fig. 5b, from 1.2 MAmp to less than 0.1 MAmp in 1.0 msec. The disruption rate is 1 MAmp/msec, at the upper limit of experimentally observed rates in tokamaks. The limiter safety factor q remains above 3 during the disruption, except at the very end. The coils are all short-circuited. The induced voltage at a point 25 mm below the center of the fast coil is shown in Fig. 5c. The voltage is initially positive due to the plasma current decrease, then negative as the plasma moves upwards, then highly positive (+400 volts) as the current disappears in the nearby plasma. If the plasma had become ideally unstable, much higher voltages might be produced (17). In Fig. 5d, the induced current in a short circuited, low resistance, fast coil is shown, which finishes with 10 KAmps, a small fraction, 1%, of the initial plasma current. Most of the rest of the initial plasma current is flowing in the vessel walls. The induced current in the fast coil, about equal to its normal operation maximum current, is small because of the small coil cross section, 25 mm x 25 mm, giving high self-inductance, and its nearness to the vessel wall. For this reason, it is not effective as a passive stabilizer, but is effective actively.

A disruption of the same plasma was simulated with up/down symmetry imposed, resulting in the same final current induced in the fast coils, assuming they are independent short cirucits, but with unidirectional current and voltage during the disruption, and lower maximum voltage values.

For vertical disruptions lasting much less time than the vessel time constant, only a small net vertical force is produced on the vessel, since the flux distribution outside the vessel is practically unchanged. A large net vertical force is produced by induced toroidal currents in the

9

vessel if the disruption time is comparable to the vessel time, and if the plasma moves vertically. An example of this is shown in Fig. 6 with plasma current in Fig. 6a, and the vertical position of the magnetic axis in Fig. 6b. The disruption rate was slowed down to 0.2 MAmp/msec by adjusting the simulation parameters to give values similar to typical experimental values in tokamaks. During the disruption, the vertical position changes considerably before the plasma current falls significantly (Figs. 6a and 6b). The flux surfaces evolve similarly to Fig. 5a. The net vertical force is found by vectorially adding the vertical forces on all the individual elements used to model the vacuum vessel. At time 2.7 msec, the net vertical force is nearly zero. However, at time 5.5 msec, the vertical force is 170 kilonewtons, the maximum observed, contrasting with nearly zero force for fast current decays. The distribution around the vessel shows the strongest force concentration occuring near the upper, small major radius corner of the vessel in the top and inner vessel wall.

On this time scale, the fast coils' resistance, connection, and protection circuitry determine the maximum induced currents. If the fast coils have zero resistance, are independent of each other, and short circuited, then at time 5.5 msec, the maximum (absolute value) induced current in either of the coils is 26 KAmp and the vertical force is 14 kilonewtons. If the resistance of each coil is a standard value of 5 mohms, then the maximum current is restricted to 7 KAmp and the force to 5 kilonewtons, occuring at 4 msec.

6.   DISRUPTION FORCES DUE TO POLOIDAL CURRENTS INDUCED IN THE VESSEL

A plasma disruption will induce poloidal currents in the vessel due to plasma paramagnetism or diamagnetism, but this current is continuous top and bottom, and does not produce a net vertical force in an up-down symmetric vacuum vessel. However, an additional vertical force has been experimentally observed, for example in JET (21). This additional force can affect the growth rate and resulting voltages, currents, and forces from the disruption, and is therefore discussed here as relevant to control system and passive stabilizer design. A differential toroidal field was measured during a vertical disruption, showing the presence of non-symmetric poloidal current in the vessel. Attempts have been made to explain this current (22), in which it was assumed that plasma motion provided the source for driving poloidal currents through a section of the vessel, closing through the plasma. Plasma resistivity was taken to be much less than the vessel resistivity in (22). Another model considers the effects of finite plasma pressure or of current flowing in the vessel(23).

In the model proposed here: 1. during a disruption, the plasma resistivity is high and may be comparable to, or greater than, the vessel resistivity; 2. the plasma pressure and beta are approximately zero, so current flow follows the field lines; 3. when the plasma intersects the wall, the wall "short-circuits" the plasma scrape-off, and carries current as if it were part of the plasma edge; 4. an additional net force on the vacuum vessel results from the interaction of the poloidal component of this current with the toroidal magnetic field. An opposite force acts on the plasma.

10

Before a disruption, the plasma has a high temperature and an established current distribution and associated stored magnetic energy. When it moves against a limiter, the edge is cooled, the plasma scraped off, and current redistributed into the hot, low resistivity plasma. The disruption in JET is accompanied by a thermal quench (24), where the temperature falls to 5 eV, and the loop voltage increases to 300 volts/turn and the plasma resistance to 400 μohm. The vessel total poloidal resistance is 32 μohm. Even when increased by an order of magnitude due to carbon tiles, supports, etc, it is comparable to the plasma. The plasma temperature and hence toroidal current density will probably be uniform, since energy loss is dominated by radiation rather than transport. In this case, the poloidal field increases (in a circular plasma) linearly with radius, and the poloidal current density increases linearly with radius, becoming maximum near the edge.

The production of large poloidal currents near the plasma edge has been observed with the TSC code in simulations of disruptions in PBX-M experiments (25), where the amount of poloidal current near the plasma edge greatly increases after the plasma temperature decreases and the plasma shrinks.

When the plasma edge region runs into the vessel wall after a disruption, unlike with a high temperature plasma, the wall resistivity is lower than the plasma it replaces, so currents, both poloidal and toroidal, continue to flow just as before in the plasma edge region, but now closing through the vessel wall. There is a dense cold plasma at the wall, so enough electrons should be available for current transfer across the boundary. In a circuit analogy, it is as if a portion of a secondary inductor, the vessel, with zero initial current, shorts out a portion of a primary, the plasma, carrying full initial poloidal and toroidal currents. Thus as the plasma current decreases, currents are symmetrically induced in the vessel as before, but there is additionally a local asymmetric current in the vessel where part of the initial current flow is transferred from part of the plasma scrape-off layer.

For example, if the plasma top touches the vessel top, the unbalanced poloidal currents provide a vertical force in one direction for the vessel and the opposite direction for the plasma. For a vertically (or radially) unstable plasma, the plasma may be expected to move vertically (or radially) until enough current is transferred to the vessel to stop plasma motion. These effects are observed in JET (21), where the plasma moves vertically and then reaches a maximum height. An up/down imbalance is measured in the toroidal field inside the vessel, implying local poloidal currents. The plasma then moves inwards and downwards, consistent with: 1. the inward motion due to decreasing current in the plasma with fixed vertical field; 2. the downward curving inner vessel corner and downward additional force.

The thickness of the scrape-off layer, d, required to provide this current may be estimated as follows: For a circular, large aspect ratio $A = R/a$ tokamak plasma, at the plasma edge, B_{pol}/B_{tor} equals $1/Aq$, where $Aq = 2\pi a B_{tor}/\mu_0 I_{tor}$. In a force-free zero-pressure plasma, where $\mathbf{J} \times \mathbf{B} = 0$, J_{pol}/J_{tor} also equals $1/Aq$. In a cold plasma with uniform temperature and flat current profile, J_{tor} equals $I_{tor}/\pi a^2$. The poloidal current component in the scrape-off layer

is $I_{scr} = 2\pi R d J_{pol}$. The experimentally measured up/down imbalance in the toroidal field is δB_{tor}. The corresponding vessel current is $I_{pol} = 2\pi R \delta B_{tor}/\mu_o$. Setting the scrape-off current I_{scr} equal to the vessel current I_{pol} gives $d = \delta B_{tor} / \mu_o J_{pol}$, or equivalently,

$$(d/a) = 2 B_{tor} \delta B_{tor} (\pi a/\mu_o I_{tor})^2 .$$

Referring to JET shot 15100, using Figs. 5,6, and 8 from Ref. (21), at time 50.055 sec, the plasma is taken to be circular with $R = 3$ m, $a = 1$ m, $I_{tor} = 2.4$ MAmps, $B_{tor} = 1.8$ T, and $\delta B_{tor} = 0.04$ T, which also gives approximate force balance. This measured δB_{tor} gives $I_{pol} = 0.6$MAmps, which is 25% of the toroidal current and 17% of the initial pre-disruption plasma current of 3.5 MAmps. The calculated thickness of the scrape-off layer is $d = 0.16$ m.

To verify that enough current can cross the scrape-off layer, note that the floating potential, typically $4 kT_e/e$, or about 20 volts, is much less than the plasma resistive voltage after a disruption. The ion saturation current density (26), if $T_e = T_i = 5$ ev, with 10^{20} /m^3 deuterium, is about 0.06 MAmps/m^2. To obtain the calculated value of I_{scr} requires a contact area with the vessel wall of 10 m^2, which with circumference $2\pi R$ gives a contact width of 0.52m, to be compared to $d = 0.16$ m. Since the scrape-off layer intersecting the vessel is nearly tangential to the wall, the contact width is plausible.

Therefore, poloidal current establishes itself to give plasma vertical force balance. There is no need to postulate a fast vertical plasma movement to drive the poloidal currents. An analytical estimate of the forces in TCV geometry using this model has not been attempted, due to the complications of calculating the forces on a highly elongated plasma. However, this model could be incorporated in TSC plasma simulations to allow for complete force balance during tokamak disruptions. For an order of magnitude estimate for TCV, if the poloidal scrape-off current flowing through the $w = 0.5$ m wide vessel top is 17% of the initial toroidal plasma current of 1.2 MAmps, as in JET, and it returns through the plasma, then the vertical force becomes $w I_{scr} B_{tor} = 150$ kilonewtons. This force will in general not add to the maximum force computed in section 5, since they occur at different values of remaining plasma current. Poloidal currents therefore provide another mechanism for producing a comparable force to that from toroidal currents.

7. SUMMARY AND CONCLUSIONS

In a non-symmetric plasma, the radial position jump caused by a pressure loss directly couples to a jump in vertical position. Although the radial motion stops after the jump, the plasma acquires a vertical velocity. The initial vertical position displacement and velocity continue to increase at the resistive growth rate. This behavior imposes certain requirements on the feedback system.

Several plasma configurations have been studied with the stabilization system of coils in the

vessel corners. It is possible to stabilize centered (vertically) and non-centered, up-down symmetric and non-symmetric plasmas with very high growth rates, much greater than $(1\,msec)^{-1}$, for example 2/1 and 3/1 elongated dee, racetrack, and single-null divertor. Even with coils only in the corners, which produce an up-down symmetric, highly distorted field in the presence of the vessel, the plasma motion can be stabilized, without visible plasma distortion. Also, higher order axisymmetric modes for plasmas up to 3/1 elongation are not observed to be dangerous on the time scale of a few msec. Pressure or apparent perturbations due to sawteeth or programmed motion, both corresponding to a 10 m/sec velocity, can be controlled with two fast power supplies on the two fast coils giving about +-50 volts/turn and +- 10 KAmp-turn for TCV.

During disruptions, the vertical position can change considerably before the plasma current falls significantly, which maximizes the net vertical force on the vessel. Near the end of such a disruption of a 1200 KAmp plasma in TCV, the vertical force due to induced toroidal currents in the vessel is 170 kilonewtons.

After the temperature quench in a disruption, the current flows along the field lines in a force-free plasma. The plasma resistivity is large, so there is no conservation of toroidal flux in the plasma. The plasma leans against the wall so that flux surfaces of the outer plasma zone intersect the walls. A helical current is enforced by the large loop voltage of the current quench, and the poloidal current component of the intersected zone is driven through the vessel, returning through the plasma. This current establishes itself automatically to give plasma vertical force balance. This model could be incorporated in a complete force balance simulation.

ACKNOWLEDGEMENTS

REFERENCES

(1)   MARCUS, F.B., JARDIN, S.C., HOFMANN, F., Phys. Rev. Lett. 55 (1985) 2289.

(2)   JARDIN, S.C., POMPHREY, N., DELUCIA, J., J. Comp. Phys. 66 (1986) 481.

(3)   HOFMANN, F., MARCUS, F.B., TURNBULL, A.D., Plasma Phys. & Cont. Fus. 28 (1986) 705.

(4)   HOFMANN, F., JARDIN, S.C., MARCUS, F.B., PEREZ, A., TURNBULL, A.D., Fusion Tech., CEC, 1 (1986) 687.

(5)   HOFMANN, F., TURNBULL, A.D., MARCUS, F.B., Nucl. Fusion 27 (1987) 743.

(6)   DELUCIA, J., HOFMANN, F., JARDIN, S.C., KELLER, R., MARCUS, F.B., et al., 13th Eur. Conf. Cont. Fusion and Plasma Physics, Schliersee (1986), Europhysics Conference Abstracts Vol. 10C, Part I (1986) 49.

(7)   MARCUS, F.B., HOFMANN, F., TONETTI, G., JARDIN, S.C., "Simulation of Plasma Evolution and Shape Control in the TCV Tokamak", Lausanne Report LRP 342/88, Switzerland (1988).

(8)   MARCUS, F.B., HOFMANN, F., JARDIN, S.C., et al., 15th Eur. Conf. Cont. Fusion and Plasma Physics, Dubrovnik (1988), Europhysics Conference Abstracts, Vol. 12B, Part I (1988) 405.

(9)   HOFMANN, F., SCHULTZ, C.G., 16th Eur. Conf. Cont. Fusion and Plasma Physics, Venice (1989), Europhysics Conference Abstracts Vol. 13B, Part I (1989) 335.

(10)   TURNBULL, A.D., ROY, A., SAUTER, O., TROYON, F.S., Nucl. Fusion 28 (1988) 1379.

(11)   SCHULTZ, C.G., BONDESON, A., TROYON, F., ROY, A., 16th Eur. Conf. Cont. Fusion and Plasma Physics, Venice (1989), Europhysics Abstracts Vol. 13B, Part I (1989) 339.

(12)   YOKOMIZO, H., NAGAMI, M., SHIMADA, M., et al., Nucl. Fusion 22 (1982) 797.

(13)   MARCUS, F.B., BAKER, D.R., LUXON, J.L., Nucl. Fusion 21 (1981) 859.

(14)   LISTER, J.B., MORET, J.-M., LAZARUS, E.A., KELLMAN, A.G., TAYLOR, T.S., FERRON, J.R., 16th Eur. Conf. Cont. Fusion and Plasma Physics, Venice (1989), Europhysics Conference Abstracts Vol. 13B, Part I (1989) 111.

(15)   MORI, M., SUZUKI, N., SHOJI, T., et al., Nucl. Fusion 27 (1987) 725.

(16)   LAZARUS, E.A., NEILSON, G.H., Nucl. Fusion 27 (1987) 383.

(17)   JARDIN, S.C., DELUCIA, J., OKABAYASHI, M., et al., Nucl. Fusion 27 (1987) 569.

(18)   PFEIFFER, W., MARCUS, F.B., ARMENTROUT, C.J., JAHNS, G.L., PETRIE, T.W., STOCKDALE, R.E., Nucl. Fusion 25 (1985) 655.

(19)   POMPHREY, N., JARDIN, S.C., WARD, D.J., Nucl. Fusion 29 (1989) 465.

(20)   WESSON, J.A., GILL, R.D., HUGON, M., et al., Nuclear Fusion 29 (1989) 641.

(21)   NOLL, P., SONNERUP, L., FROGER, C., HUGUET, M., LAST, J., "Forces on the JET Vacuum Vessel During Disruptions and Consequent Operational Limits", ANS Topical Meeting Tech. Fusion Energy, Salt Lake City (Oct. 1988).

(22)   JENSEN, T.H., CHU, M.S., "Long Term Development of Elongated Tokamak Plasmas after Failure of the Feed-back Stabilizing Circuit", General Atomics Report GA-A19277 (1988), submitted to Phys. Fluids.

(23) ALBANESE, R., BERTOLINI, E., BOBBIO, S., MARTONE, R., MIANO, G., NOLL, P., "Analysis of
      Vertical Instability in the JET Experiment", 15th Symposium on Fusion Tech., Utrecht
      (Sept. 1988).

(24) WARD, D.J., GILL, R.D., MORGAN, P.D., WESSON, J.A., 15th Eur. Conf. Cont. Fusion and
      Plasma Physics, Dubrovnik (1988), Europhys. Conf. Abstracts, Vol. 12B, I (1988) 405.

(25) KUGEL, H.W., ASAKURA, N., BELL, R., et al., 16th Eur. Conf. Cont. Fusion and Plasma
      Physics, Venice (1989), Europhysics Abstracts Vol. 13B, Part I (1989) 199.

(26) VON ENGEL, A., Ionized Gases, Oxford University Press (1965) 296.

TABLE 1. FEEDBACK CONTROL OF PRESSURE PERTURBATIONS

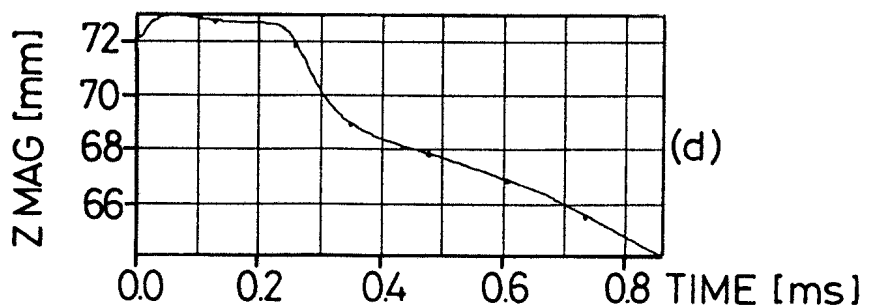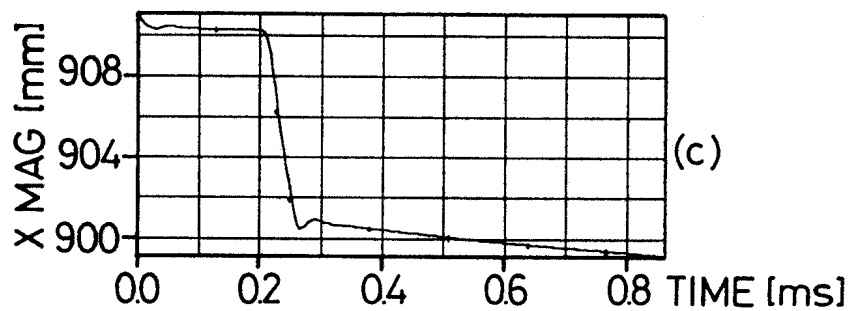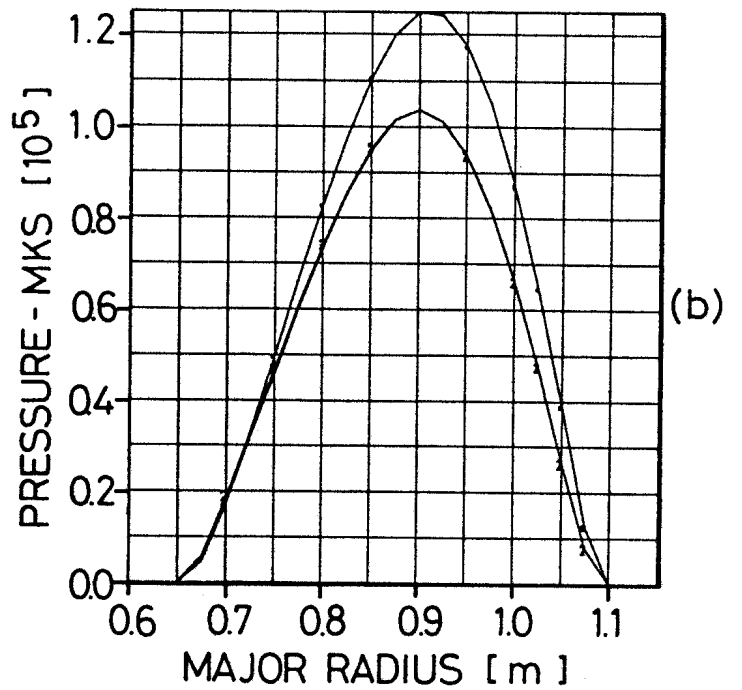| $\Delta\beta$	Δt_J	R_c	ΔI_c	$-\Delta R$	$-\Delta z$
%	msec	mΩ	kA	mm	mm
0.25	0.05	5.	4	3	1
0.50	0.05	5.	7	6	2
1.0	0.05	0.05	18	12	4-6*
1.0	1.00	0.05	11	11	3

*overshoot

Fig. 1. (case 940) plasma response in the absence of feedback; (1a) a 2.2/1 elongated, single-null divertor equilibrium in TCV geometry. (1b) before and after radial profiles of pressure; (1c) radial and (1d) vertical time response of the position of the plasma magnetic axis.

Fig. 2. (case 943) feedback control using only rapid coils. β is dropped from 5.8% at to 5.3%; (2a) vertical position of the magnetic axis versus time; (2b) the applied voltage and (2c) resulting current waveforms of the upper feedback coil.

Fig. 3. (cases 915,950) initial MHD equilibrium with $\kappa=3/1$ and $I_p = 1200$ KAmps calculated with TSC for studying control of programmed motion.

Fig. 4. (case 950) plasma control of programmed plasma motion with both fast and slow coils; (4a) plasma and coil geometry, where snapshots of the lower portion of the outermost flux surface show the bottom of the plasma moving upwards; (4b) the bottom fast coil voltage and (4c) resulting fast coil current; (4d) voltage and (4e) current on the bottom shaping coil at large major radius; (4f) the vertical position of the magnetic axis.

Fig. 5. (case 1051) rapid current loss and vertical disruption; (5a) snapshots of the outermost flux surface; (5b) plasma current; (5c) the induced voltage at a point 25 mm below the center of the fast coil; (5d) the induced current in the short circuited fast coil.

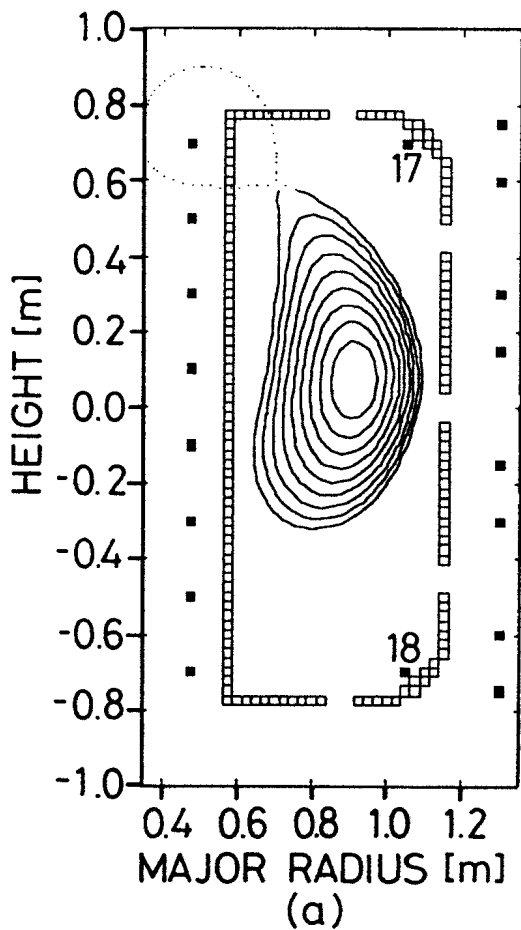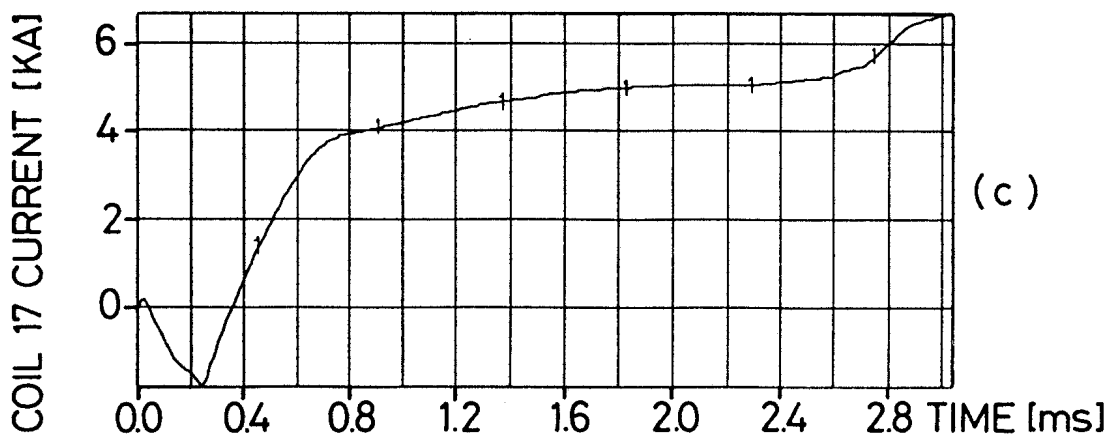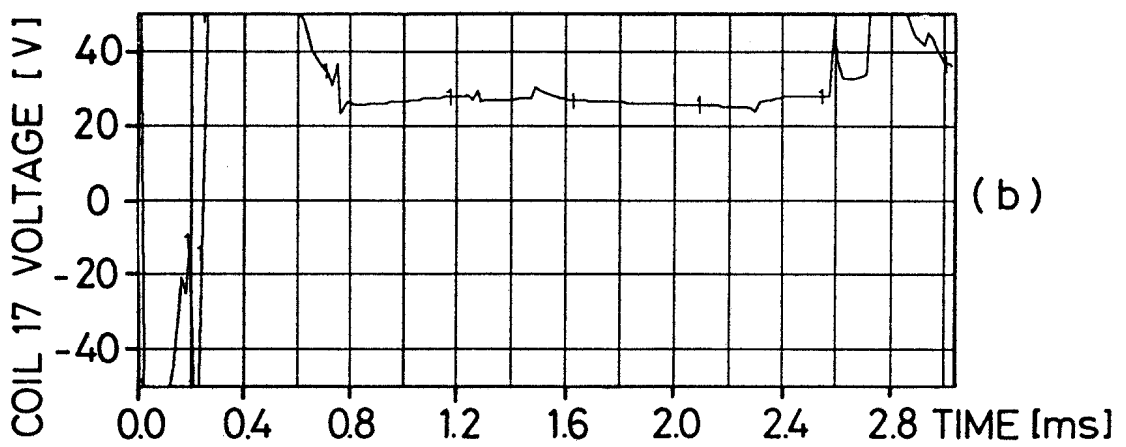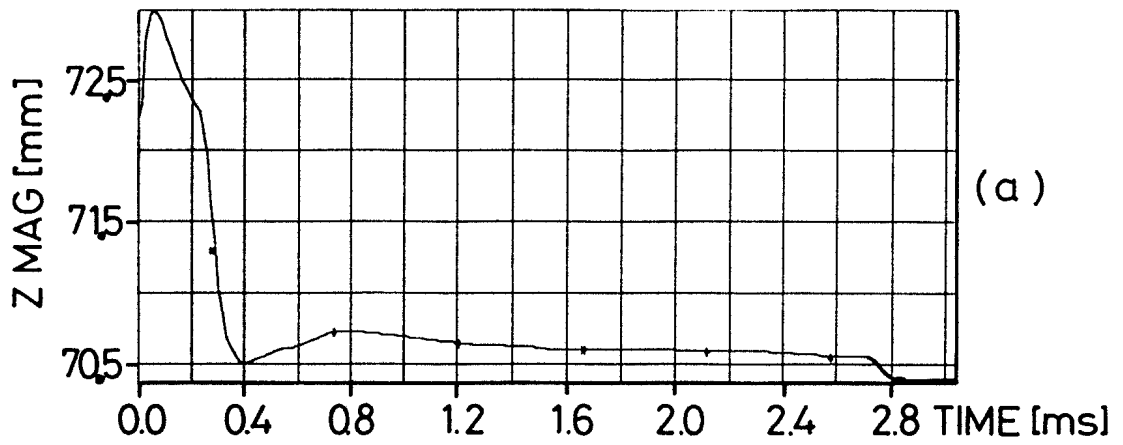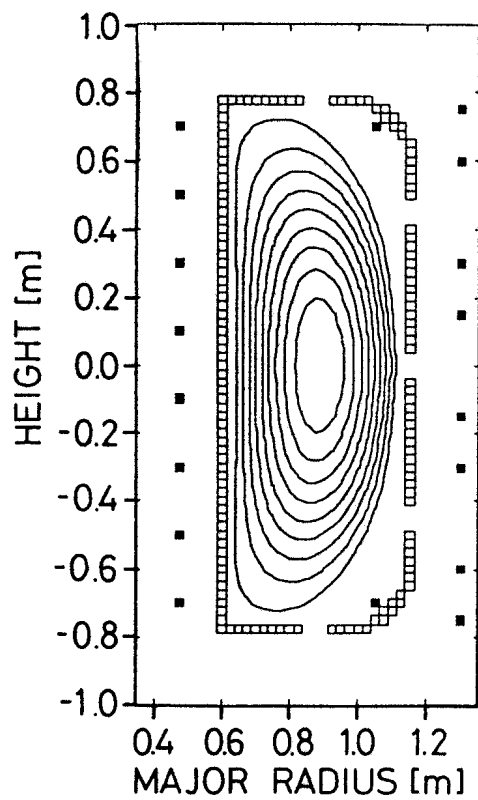Fig. 6. (case 1060) slow, non-symmetric disruption; (6a) plasma current; (6b) vertical position of the magnetic axis.

Fig. 1. (case 940) plasma response in the absence of feedback; (1a) a 2.2/1 elongated, single-null divertor equilibrium in TCV geometry. (1b) before and after radial profiles of pressure; (1c) radial and (1d) vertical time response of the position of the plasma magnetic axis.

Fig. 2. (case 943) feedback control using only rapid coils. β is dropped from 5.8% at to 5.3%;
(2a) vertical position of the magnetic axis versus time; (2b) the applied voltage and (2c)
resulting current waveforms of the upper feedback coil.

Fig. 3. (cases 915,950) initial MHD equilibrium with $\kappa=3/1$ and I_p = 1200 KAmps calculated with TSC for studying control of programmed motion.
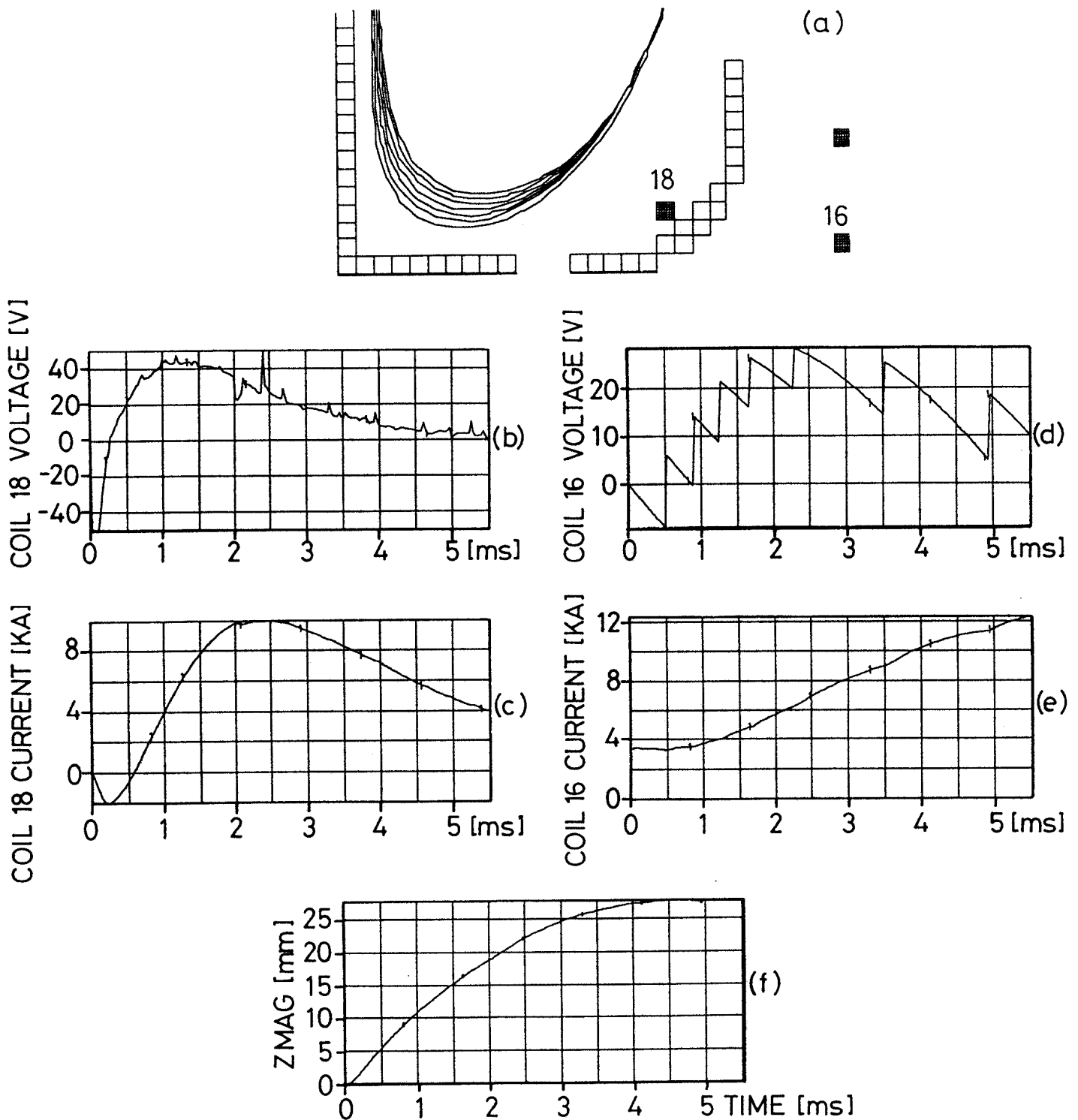
Fig. 4. (case 950) plasma control of programmed plasma motion with both fast and slow coils; (4a) plasma and coil geometry, where snapshots of the lower portion of the outermost flux surface show the bottom of the plasma moving upwards; (4b) the bottom fast coil voltage and (4c) resulting fast coil current; (4d) voltage and (4e) current on the bottom shaping coil at large major radius; (4f) the vertical position of the magnetic axis.
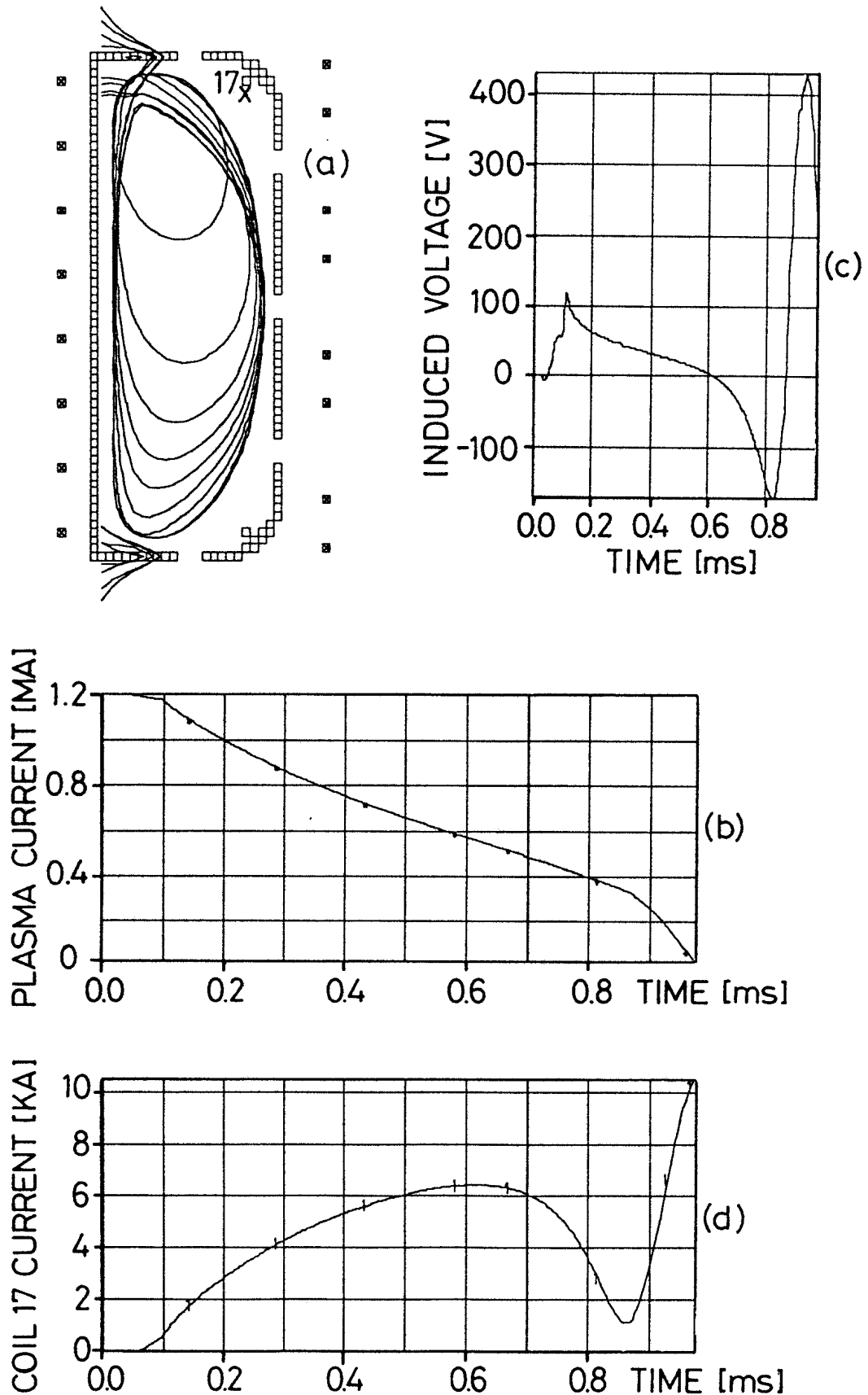
Fig. 5. (case 1051) rapid current loss and vertical disruption; (5a) snapshots of the outermost flux surface; (5b) plasma current; (5c) the induced voltage at a point 25 mm below the center of the fast coil; (5d) the induced current in the short circuited fast coil.
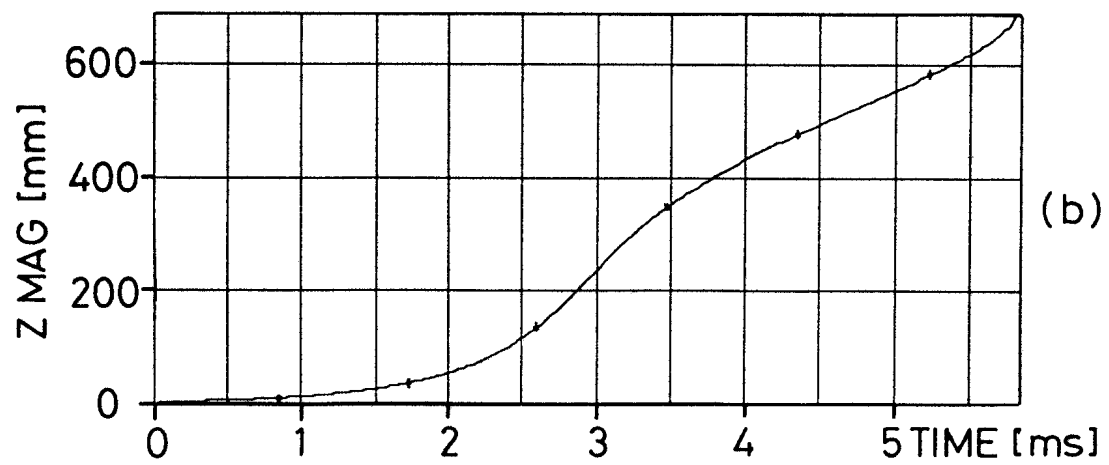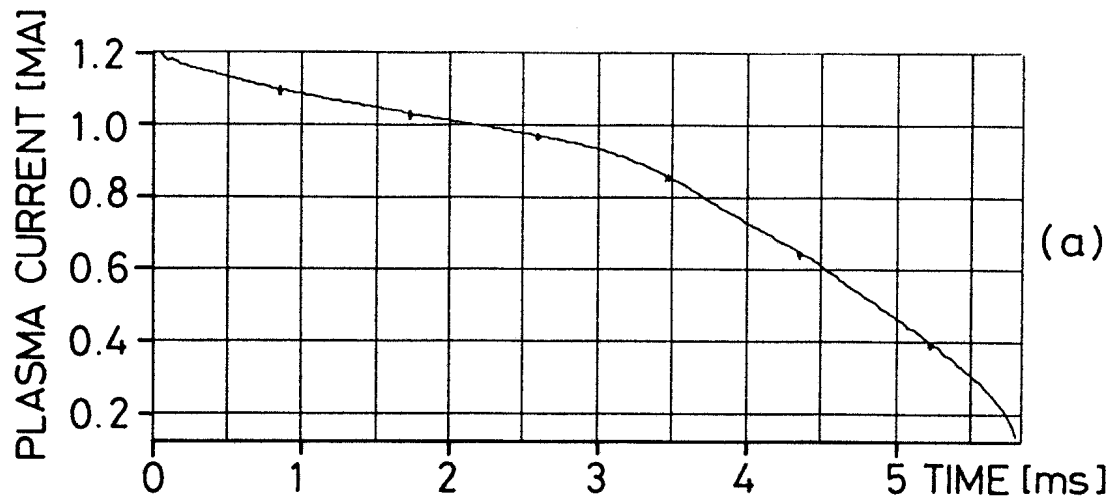
Fig. 6. (case 1060) slow, non-symmetric disruption; (6a) plasma current; (6b) vertical position of the magnetic axis.